An Experimental and ab Initio Study of Hypervalent LiOZn

Zheng-Wen Fu, Lu−Ning Zhang, and Qi-Zong Qin*

Laser Chemistry Institute, Fudan University, Shanghai 200433, People's Republic of China

Yi-Hua Zhang and Xiang-Kang Zeng

Chemistry Physics Laboratory, East China University of Science and Technology, Shanghai 200237, People's Republic of China

Hong Cheng, Rong-Bin Huang, and Lan-Sun Zheng

State Key Laboratory for Physical Chemistry of the Solid Surface, Xiamen University, Fujian 361005, People's Republic of China

Received: October 28, 1999; In Final Form: January 10, 2000

An unusual intercalation of lithium zinc oxide (LiZnO) is produced by the electrochemical lithium insertion into a ZnO film electrode. As its isolated unit, LiOZn and $LiOZn^+$ molecules exhibit a new type of hypervalent species with two heterometal atoms and one oxygen atom. Time-of-flight mass spectrometry has also been employed to give direct experimental evidence for the existence of $LiOZn^+$ generated by laser ablation of a composite Li/ZnO target in a high vacuum. The stability and structure of the hypervalent molecule LiOZn and its ion as well as its isomer are investigated by ab initio molecular orbital calculations. The overlap between the 2s orbital in Li, the $2p_y$ orbital in O, and the 4s orbital in Zn should be responsible for a linear structure of these molecules. The extra one electron beyond the usual octet in LiOZn may play an important role in the binding between a lithium atom and a zinc atom around the central oxygen atom.

1. Introduction

As a formal octet rule for some thermodynamically stable molecules, elements in the second row of the periodic table normally prefer to be surrounded by eight electrons. Since the experimental discovery of OLi_3 and OLi_4 molecules in the early 1980s, these molecules with nine and more valence electrons, so-called hyperlithiated or hypervalent molecules, have received much attention.[1] Subsequently, many experimental works exhibit more polylithiated molecules such as CLi_5, CLi_6, Li_3S, Li_4S, Li_4P, $SiLi_4$, and Li_2CN.[2−12] In the meantime, ab initio calculations provide important information about the stability and structure of these molecules with unusual stoichiometry. Previous investigations suggested that some molecules containing lithium and main-group elements may exceed the normal valence expectation, while they are thermodynamically stable toward loss of lithium. The investigations about hypervalent molecules, however, have not been satisfactorily carried out yet. It is a challenge to identify the existence of new hypervalent molecules because of their structural flexibility and the difficulty of forming these stable molecules.

Previous reports on the hypervalent molecules mainly focused on the polyatomic molecules with more than three atoms such as Li_3O, Li_4O, Li_3S, and Li_2CN as we mentioned above.[1−12] To our knowledge, little information is available on hypervalent molecules involving only three atoms with two different metal atoms and one oxygen atom. Although we have recently reported the experimental observation and theoretical prediction of the existence of the LaOMn and $LaOMn^+$ generated by pulsed laser ablation of a $La_{0.33}Ca_{0.67}MnO_3$ target,[13] the characteristics of hypervalent molecules are not investigated in detail. In this paper, we first present the existence of a new type of hypervalent molecules, LiOZn and $LiOZn^+$, by the lithium intercalation electrochemical reaction and gas-phase ion−molecule reactions. They are identified by the spectroelectrochemical method and time-of-flight mass spectrometry, respectively. Meanwhile, ab initio calculations will also be used to predict the structure and stability of these hypervalent molecules.

2. Experimental Section

The experiments for the investigation of hypervalent molecules mainly involve two parts: a spectroelectrochemical measurement and laser plasma time-of-flight (TOF) mass spectrometry. The detailed descriptions about two experimental methods have been reported previously.[14,15] Here, these two methods are described briefly as follows.

Spectroelectrochemical measurements were carried out in a conventional three-electrode cell with a ZnO film deposited on the coated indium−tin oxide (ITO) glass by pulsed laser deposition as a working electrode[14] and two sheets of high-purity lithium metal as the counter electrode and reference electrode, respectively. The electrolyte consisted of 1 M $LiPF_6$ in a nonaqueous solution of ethylene carbonate (EC) and dimethyl carbonate (DMC) with a volume ratio of 1:1 (Merck). The electrochemical cell consisted of one pair of glass windows with an H-type tube, in which the counter electrode and reference electrode were placed. A couple of quartz windows were sealed in another tube with the working electrode; the detected light beam with a diameter of about 4 mm passed through the quartz window and was focused on the ZnO film electrode surface normal. Cyclic voltammetric measurement was carried out with a CHI 660a electrochemical working station (CHI Instruments, TN). In situ transmittance spectra of the

10.1021/jp993834g CCC: $19.00
Published on Web 03/11/2000

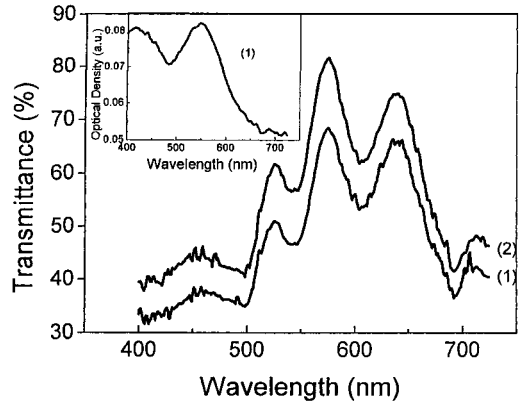

Figure 1. In situ transmittance for the ZnO film electrode in the wavelength range from 400 to 700 nm during cyclic voltammetry (1) in the colored state (at 1.0 V) and (2) in the bleached state (at 3.0 V). The absorbance in the colored state (LiOZn) is shown in the inset

electrochemical cell including quartz windows, electrolyte, and working electrode were measured by a SM-210 charge-coupled device (CCD) spectrophotometer (CVI Spectral Instruments, Putnam, CT).

A laser plasma/TOF mass spectrometric system consisted of an ablation chamber and homemade TOF mass spectrometer. A 532 nm beam was provided by the second harmonic frequency of a Q-switched Nd:YAG laser, and passed through the acceleration zone in a direction perpendicular to the acceleration field and then was focused onto a Li/ZnO composite target with a laser power density of $\sim 10^8$ W/cm^2. The laser-ablated species entered into the acceleration zone by their initial kinetic energy, and were accelerated by a pulsed high-voltage electric field of 950 V. The accelerated ablated ions then entered a field-free drift tube, and their masses were analyzed by the flight time. The time delay (t_d) between the ablation laser pulse and high-voltage extraction pulse was controlled by a pulse delay generator. The ions were detected by a dual microchannel plate, and the signals fed into a transient recorder interfaced to a computer. Each TOF mass spectrum was recorded by averaging over 50 laser pulses.

3. Results and Discussion

3.1. Lithium Intercalation Reaction. It is well-known that the electrochemical reaction offers a convenient possibility to obtain new compounds. For example, the intercalation of a monovalent ion (H^+, Li^+, Na^+) into metal oxides during cathodic polarization leads to the formation of an intercalation compound such as $LiTiO_2$ and $LiWO_3$.[16,17] Recently, our laboratory has fabricated a high-quality *c*-axis-oriented nanocrystalline ZnO film onto a coated ITO glass using pulsed laser deposition, and examined the electrochemical behaviors of lithium intercalation into a ZnO film.[14]

Figure 1 shows in situ transmittance spectra of the ZnO electrode in the wavelength range from 400 to 700 nm recorded at 1 and 3 V, respectively, with a scan rate of 5 mV during cyclic voltammetry. All potentials are with regard to a Li/Li$^+$ electrode. It can be seen that the transmittance of the ZnO film electrode is large at the potential of 3 V, and the electrode is in the bleached state. The Li ion is not inserted into ZnO film in this state. However, the transmittance of the ZnO electrode decreases at the potential of 1 V, and the electrode is in the colored state, corresponding to the intercalation of Li ion into the ZnO film. The optical density spectrum of the colored state (LiZnO) is shown in the inset of Figure 1. Two absorption peaks around 410 and 550 nm are observed. These results can be explained by the electrochemical behaviors with the intercalation process of Li ions into the ZnO film electrode.

Zinc oxide is a wide band gap semiconductor with a band gap close to 3.2 eV, and is hence transparent in the visible region. It is interesting to note that Li ion intercalation into the ZnO film gives rise to a strong color change. This evidence strongly proves that an unusual intercalation of lithium zinc oxide with color is formed by the intercalation reaction of ZnO and Li ion, which can be represented by

$$\mathrm{ZnO\ (colorless)} + x(\mathrm{Li^+} + \mathrm{e^-}) \rightarrow \mathrm{Li}_x\mathrm{ZnO\ (colored)}$$

where e^- denotes the charge-balancing electron and x is the so-called intercalation coefficient. However, the process for Li intercalation into metal oxides is rather complicated and may be related to the physical features of host material such as the morphology and the structure.[18−20] For the case of lithium intercalation into a ZnO lattice, the above chemical reaction can be easily considered as follows: when Li ions are incorporated into the ZnO lattice under the conditions of the lithium insertion potential, and close to the O atom or the Zn−O bonding in the ZnO lattice, the solid-state reaction between Li ion and its adjacent ZnO occurs. At the same time, one part of the injected electrons take part in such a chemical reaction to produce LiZnO. In addition, the other part of the charge-balancing electrons may be trapped in the defects of the solid-state film, and do not partake in the reaction between Li^+ ion and ZnO, which will lead to the formation of $LiZnO^+$. Thus, the spectroelectrochemical result shows a nonstoichiometric intercalation of LiZnO, and implies the existence of LiZnO and $LiZnO^+$ species.

3.2. Ion−Molecule Reaction in Laser Ablation Plasma. Laser ablation of an appropriate sample is a valuable method for generating hypervalent molecules. Wang et al.[21] reported the observation of hypervalent molecules K_2CN and K_2CN^+ generated by 266 nm pulsed laser ablation of solid $K_3Fe(CN)_6$. Here, we investigate 532 nm laser ablation of a composite target made from metallic lithium and ZnO in a high vacuum, and time-of-flight (TOF) mass spectrometry was employed for searching for a new hypervalent molecule, $LiOZn^+$.

Figure 2a shows a TOF mass spectrum of positive ions at the delay time of 10 μs for the laser ablation of a composite Li/ZnO target. It can be seen that besides the signals for the mass number (m/e) < 64 with relative abundance, the m/e = 64, 65, and 66 signals can be assigned to the natural isotopic peaks for the Zn atom. It should be noted that there is a clear signal for the mass number 87, which is in agreement with the sum of the mass numbers of Li (7), O (16), and Zn (64), and could be attributed to $LiZnO^+$, but other possibilities are not excluded. Therefore, an experiment has also been done using a metallic lithium target instead of a composite Li/ZnO target under the same experimental conditions. As shown in Figure 2b, the TOF mass spectrum in the m/e < 64 region for the laser ablation of a metallic lithium target is the same as that in Figure 2a measured with a composite Li/ZnO target. These signals can be attributed to Li^+ (m/e = 6), Li^+ (m/e = 7), Li_2^+ (m/e = 13), Li_2^+ (m/e = 14), LiO^+ (m/e = 22), LiO^+ (m/e = 23), Li_2O^+ (m/e = 29), Li_2O^+ (m/e = 30), Li_3O^+ (m/e = 36), Li_3O^+ (m/e = 37), Li_4O^+ (m/e = 44), and Li_4O^+ (m/e = 45). The existence of isotopic peaks for lithium and its compounds also supports these assignments. Since the metallic lithium target can be easily oxidized before the laser ablation and form a lithium oxide layer on the target surface, it leads to the presence of many lithium oxide molecules such as Li_3O^+ and Li_4O^+ hypervalent molecules in the laser ablation process. These molecules have been recently

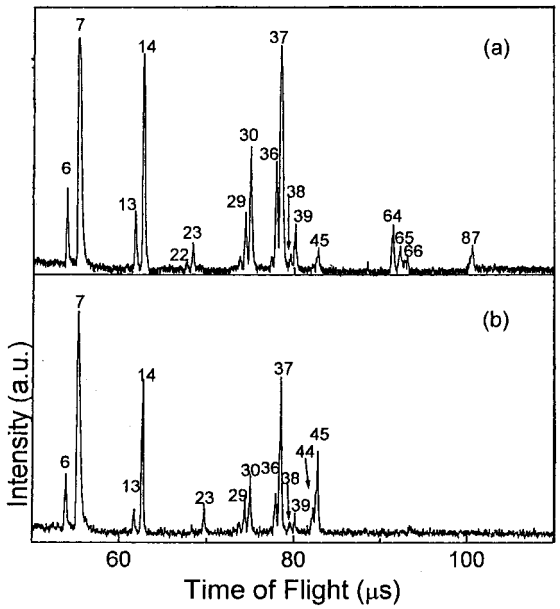

Figure 2. Time-of-flight mass spectra of measured positive ions for 532 nm laser ablation of two different targets: (a) Li/ZnO; (b) Li. Laser power density $\sim 10^8$ W/cm^2. Delay time 10 μs.

studied by Lievens at al. using a laser vaporization source and a TOF mass spectrometer.[12] It should be noted that no peak is detected at mass numbers of more than 64 for the laser ablation of the metallic lithium target. In addition, the signals of Zn^+ ($m/e = 64$), Zn^+ ($m/e = 65$), and Zn^+ ($m/e = 66$) appeared in a TOF mass spectrum measured from another experiment, in which a pure ZnO target was used for the laser ablation under the same experimental conditions (not shown in Figure 2). By comparison of these results, the signal at $m/e = 87$ in Figure 2a should be assigned to a hypervalent molecule, $LiOZn^+$, which is formed by ion−molecule reaction between lithium and zinc oxide in laser ablation plasma. It should be noted that ZnO^+ ions are absent in the plasma from the TOF mass spectrum of positive ions; this could be attributed to the high ionization potential of ZnO.

The dependencies of the signal intensities of $LiOZn^+$ and Zn^+ on the delay time (t_d) are measured for further examining the formation of $LiOZn^+$. Figure 3a shows the TOF mass spectra observed at different delay times. It can be seen that the formation of $LiOZn^+$ in laser ablation plasma depends on the delay time, and the hypervalent molecule $LiOZn^+$ is observed obviously at the delay time from 7.5 to 17.5 μs. For comparison, the relative intensities or relative ablated yields for $LiOZn^+$ and Zn^+ obtained by integrating their peaks are estimated as a function of (t_d). As shown in Figure 3b, the relative intensity for $LiOZn^+$ increases gradually with increasing t_d, while there is a maximum at 10 μs for Zn^+. This result implies that there are two different processes for generating $LiOZn^+$ and Zn^+ in laser ablation plasma. It suggests that Zn^+ ions are generated directly from the laser−target interaction, while $LiOZn^+$ may result from the ion−molecule reaction during the expansion of laser ablation plasma. Considering that Li ion may be one of the main products in the plasma because of easy ionization of Li atoms, the possible ion−molecule reactions can be suggested as

$$Li^+ + ZnO \rightarrow LiOZn^+ \quad (1)$$

$$LiO^+ + Zn \rightarrow LiOZn^+ \quad (2)$$

$$LiO + Zn^+ \rightarrow LiOZn^+ \quad (3)$$

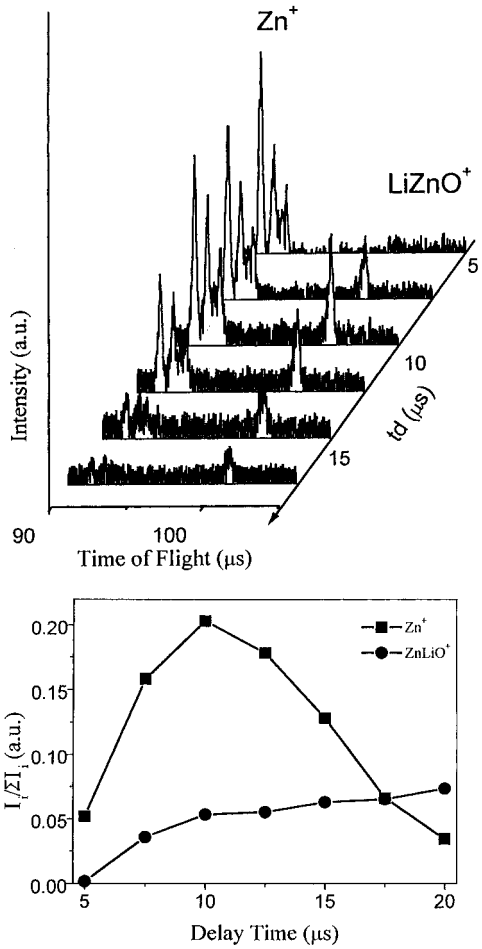

Figure 3. (a, top) Measured signals of Zn^+ and $LiZnO^+$ ions from 532 nm laser ablation of the Li/ZnO composite target at different t_d values. (b, bottom) $I_{Zn}/\sum I_i$ (■) and $I_{LiZnO}/\sum I_i$ (●) versus t_d.

Among these possible pathways, reaction 1 is in agreement with the intercalation reaction of Li ion with ZnO as we mentioned above. It should be noted that the quantity of $LiOZn^+$ is still increasing when the concentration of Zn^+ is in fact much lower as shown in Figure 3b. This result shows that the reaction of ablated Zn^+ and LiO in the plume may not be the sole pathway for the generation of $LiOZn^+$; even if the concentration of Zn^+ is much lower, the quantity of hypervalent ion will still increase via other reaction pathways.

3.3. Theoretical Calculations. To confirm the existence of hypervalent molecules LiZnO and $LiZnO^+$, ab initio calculations were performed by using the Gaussian 94 program.[22] We employed the MP2[23] and B3LYP[24,25] methods with 6-311G basis sets on Li and O atoms, and the set of Wachters and Hay for Zn.[26−27] No constraints have been set on the structures during optimization, and harmonic analysis was performed on each stationary point. Since $LiZnO^+$ has two isomers, $LiOZn^+$ and $OLiZn^+$, we have calculated the ground and low-lying excited states of $LiOZn^+$ and $OLiZn^+$ as well as their corresponding neutral molecules. As those isomers are stable in energy, the natural bond orbital (NBO) analysis[28] is useful for interpreting the electronic structures of a molecule in terms of Lewis valence bond structures. In addition, CIS (configuration interaction of single excitation) calculations[29] were also done for ground-state $LiOZn^+$, LiOZn, $OLiZn^+$, and OLiZn to assign the electronic spectra of an intercalation of the LiZnO electrode mentioned above.

The optimized structural parameters and vibrational frequencies of neutral and positively charged LiOZn and OLiZn are

TABLE 1: Optimized Geometrical Parameters and Unscaled Vibrational Frequencies of Various Structures

	MP2		B3LYP	
species (state)	geometries	frequencies	geometries	frequencies
LiOZn (^{2}A′)	LiO: 1.584. ZnO: 1.797, 179.74	125.3, 618.8, 1098.8	LiO: 1.580. ZnO: 1.852, 179.73	80.4, 427.7, 1030.7
LiOZn (^{4}A′)	LiO: 1.847. ZnO: 1.928, 179.85	128.7, 375.9, 656.2	LiO: 1.859. ZnO: 1.964, 179.66	73.2i, 321.0, 597.6
OLiZn (^{2}A′)	LiO: 1.719. LiZn: 2.852, 178.31	66.5, 100.5, 816.4	LiO: 1.601. LiZn: 2.730, 178.08	50.6i, 103.2, 890.7
LiOZn$^+$ (^{1}A′)	LiO: 1.661. ZnO: 1.774, 178.04	63.5, 519.8, 913.0	LiO: 1.654. ZnO: 1.764, 178.95	45.6, 508.5, 911.3
LiOZn$^+$ (^{3}A″)	LiO: 1.791. ZnO: 1.990, 179.21	45.6, 508.5, 911.3	LiO: 1.782. ZnO: 2.002, 179.17	121.9, 328.7, 700.9
OLiZn$^+$ (^{3}A″)	LiO: 2.161. LiZn: 2.703, 178.22	48.8, 127.2, 391.9		
OLiZn$^+$ (^{1}A′)	LiO: 2.155. LiZn: 2.702, 178.26	30.4, 126.6, 389.2	LiO: 2.118. LiZn: 2.646, 178.46	48.4, 129.7, 401.7

TABLE 2: Relative Energies of Neutral and Positively Charged LiOZn and OLiZn

	MP2/6-311G		B3LYP/6-311G	
species (state)	ΔE [a]	ΔE [b]	ΔE [a]	ΔE [b]
LiOZn (^{2}A′)	−131.2	−130.7	−151.3	−151.2
OLiZn (^{2}A′)	−107.0	−107.8	−129.2	−129.9
LiOZn (^{4}A′)	−69.1	−69.5	−81.7	−82.5
LiOZn$^+$ (^{1}A′)	0	0	0	0
LiOZn$^+$ (^{3}A″)	12.4	12.0	8.3	7.8
OLiZn$^+$ (^{3}A″)	59.1	57.8		
OLiZn$^+$ (^{1}A′)	127.6	125.4	115.8	114.6

[a] The energies of LiOZn (^{2}A′) at the MP2 and B3LYP levels are −1860.377 244 and −1862.048 170 au, respectively. [b] Relative energies corrected with ZPE.

TABLE 3: Calculated Vertical Excitation Energies (nm) and Oscillator Strengths (in parentheses) for Neutral and Positive Charged LiOZn and OLiZn

	CIS/6-311+G(d)//-MP2/6-311G			CIS/6-311+G(d)//-B3LYP/6-311G		
	state 1	state 2	state 3	state 1	state 2	state 3
LiOZn$^+$ (^{1}A′)	484.2 (0.0108)	484.1 (0.0109)	257.2 (0.1468)	474.7 (0.0112)	474.6 (0.0112)	255.2 (0.1426)
LiOZn (^{2}A′)	324.4 (0.1389)	324.4 (0.1389)	285.1 (0.0834)	327.5 (0.0741)	327.5 (0.0741)	300.6 (0.1428)
OLiZn$^+$ (^{3}A″)	1839.7 (0.0000)	1839.7 (0.0000)	515.8 (0.0000)			

summarized in Table 1. The energies of these species are listed in Table 2. It has been found that the ground state of LiOZn$^+$ is ^{1}A′. Take the MP2 results for example; a near linear structure ($a = 178.0$) was obtained with Li−O and Zn−O bond lengths of 1.661 and 1.774 Å, respectively. As can be seen in Table 1, the results at the B3LYP level are quite similar to the MP2 values. For the OLiZn$^+$ isomer, ^{3}A″ is predicted to be the ground state at the MP2 level. However, this molecule still lies 59.1 kcal/mol higher in energy than LiOZn$^+$(^{1}A″). In this isomer, the Zn atom is directly bonded to the Li atom, and the Li−Zn bond length is 2.703 Å, which is in the range of a typical metal−metal bond. We are unable to locate the ^{3}A″ OLiZn$^+$ structure with the B3LYP method. Since OLiZn$^+$ is much higher in energy than LiOZn$^+$, we believe that the formation of OLiZn$^+$ would be less thermodynamically favorable than that of LiOZn$^+$.

The neutral ^{2}A′ LiOZn is a ground state with a total energy more stable by 131.2 and 151.3 kcal/mol than LiOZn$^+$ at the MP2 and B3LYP levels, respectively. The OLiZn in the ^{4}A′ state is also a stable isomer, lying approximately 100 kcal/mol lower than OLiZn$^+$. Our results show that both neutral isomers are more stable than their corresponding positively charged states.

According to the electrochemical results, the Li ion insertion into the ZnO structure may result from the interaction between Li ion and the oxygen atom in ZnO to generate a LiOZn$^+$ structure, instead of Li ion inserting into the Zn−O bond to generate another OLiZn$^+$ structure. Thus, the intercalation compounds should mainly consist of LiOZn$^+$ and LiOZn, instead of OLiZn$^+$ and OLiZn from the energy point of view.

The singlet excitation transitions were calculated for LiOZn$^+$ and LiOZn, and their isomers. As shown in Table 3, the first electronic transition for OLiZn and OLiZn$^+$ molecules is beyond the visible wavelength with negligible oscillator strength. This means that these two molecules do not absorb the visible light. The calculated result at the MP2 level is identical to that at the B3LYP level. However, the first excitation transition of ^{1}A′ LiOZn$^+$ is located at 484 nm with a relative coefficient of 0.0108, and the first excitation transition for the ^{2}A′ LiOZn is obtained at 324 nm. Although the CIS results are qualitative at best, these values are unexpectedly close to the absorption of an intercalation compound of LiZnO, in which there are two absorption peaks centered at 410 and 550 nm. A little longer wavelength absorption of the spectroelectrochemical result compared with the calculated results may be related to the surrounding restriction of LiOZn and LiOZn$^+$ molecules in the solid-state phase.

The NBO analysis mainly focused on LiOZn$^+$ and LiOZn since these molecules are most stable. Natural population analysis on LiOZn$^+$ showed that the bond between Li and O is the consequence of overlap between the 2s orbital of Li and the 2p$_y$ orbital of O. The electron in the 2s orbital of Li has almost totally been donated to the O atom. Also, the Zn−O bond is found to be formed by the interaction between the 4s atomic orbital of Zn and the 2p$_y$ orbital of O. Comparing the electron structures of LiOZn and LiOZn$^+$, it is found that both molecules have the character of a dumbbell bond formed by head to head overlap of the 2s orbital of the Li atom, 2p$_y$ orbital of the O atom, and 4s orbital of the Zn atom, while the singly positively charged LiOZn$^+$ seems to have lost one electron total from both Li (∼0.3) and Zn (∼0.7) atoms. In both species, the atomic charge of the central O atom remains almost unchanged. According to the theoretical studies by Schleyer et al.[1] and Kudo et al.,[9] the extra electrons in such hypervalent molecules as Li$_3$O (9 valence electrons), Li$_4$O (10 valence electrons), Li$_3$S (9 valence electrons), and Li$_4$S (10 valence electrons) would contribute equally to the O−Li and O−S bonding. However, one extra electron in Li$_3$O and Li$_3$S and two extra electrons in Li$_4$O and Li$_4$S are suspected for making a main contribution to the Li−Li bonding for a metallic cage around the central oxygen or sulfur atoms. Thus, for the hypervalent molecule LiOZn (9 valence electrons) and its ion LiOZn$^+$, the overlap among the 2s orbital in Li, the 2p$_y$ orbital in O, and the 4s orbital in Zn is considered to play an important role in the linear structure of these molecules. The extra electron may make a main contribution to the binding between a Li atom and a Zn atom around the central oxygen atom.

4. Conclusion

The electrochemical reaction of the insertion of Li ion into host material has generated an intercalation LiZnO. This offers a possibility to investigate a new type of hypervalent molecule,

LiZnO, which consists of two heterometal atoms and one oxygen atom. The direct experimental evidence for the observation of $LiZnO^+$ is obtained by TOF mass spectrometry using laser ablation of a composite Li/ZnO target in a high vacuum. Ab initio calculations give the stable structures of $LiOZn^+$ and $OLiZn^+$ and their neutral molecules, and the structures of LiOZn and its ion are predicted to be more stable than those of OLiZn and its ion.

Our experimental and theoretical results confirm the existence of hypervalent molecules LiOZn and $LiOZn^+$. In both molecules, the overlap among the 2s orbital in Li, the $2p_y$ orbital in O, and the 4s orbital in Zn plays an important role in the linear structure of these molecules. The extra electron beyond the usual octet in LiOZn is considered to be involved in the binding between a lithium atom and a zinc atom around the central oxygen atom.

Finally, it should be emphasized that the electrochemical reaction of insertion of Li ion into host material will help to discover new compounds and may become a useful method for the guide to stable molecules of lithium derivatives.

Acknowledgment. This work is supported by the National Natural Science Foundation of China (Project No. 29783001).

References and Notes

(1) Schleyer, P. v. R.; Wurthwein, E. U.; Pople, J. A. *J. Am. Chem. Soc*. **1982**, *104*, 5839.
(2) Schleyer, P. v. R.; Wurthwein, E. U.; Kaufmann, E.; Clark, T. J. *J. Am. Chem. Soc*. **1983**, *105*, 5930.
(3) Schleyer, P. v. R.; Tidor, B.; Jemmis, E. D.; Chandrasekhar, J.; Werthwein, E. U.; Kos, A. J.; Luke, B. T.; Pople, J. A. *J. Am. Chem. Soc.* **1983**, *105*, 484.
(4) Schleyer, P. v. R.; Read, A. E. *J. Am. Chem. Soc*. **1988**, *110*, 4453.
(5) Read, A. E.; Schleyer, P. v. R.; Janoschek, R. *J. Am. Chem. Soc*. **1991**, *113*, 1885.
(6) Kudo, H.; Zmbov, K. F. *Chem. Phys. Lett.* **1991**, *87*, 77.
(7) Kudo, H. *Nature* **1992**, *355*, 432.
(8) Ivanic, J.; Marsden, C. J. *J. Am. Chem. Soc*. **1993**, *115*, 7503.
(9) Kudo, H.; Yokoyama, K.; Wu, C. H. *J. Chem. Phys*. **1994**, *101*, 4190.
(10) Kudo, H.; Hashimoto, M.; Yokoyama, K.; Wu, C. H.; Dorigo, A. E.; Bickelhaupt, F. M.; Schleyer, P. v. R. *J. Phys. Chem*. **1995**, *99*, 6477.
(11) Jones, R. O.; Lichtenstein, A. I.; Hutter, J. *J. Chem. Phys*. **1997**, *106*, 4566.
(12) Lievens, P.; Thoen, P.; Bouckaert, S.; Bouwen, W.; Vanhoutte, F.; Weidele, H.; Silverans, R. E.; Vazquez, A. N.; Schleyer, P. v. R. *J. Chem. Phys*. **1999**, *110*, 10316.
(13) Wang, X. F.; Dang, H. J.; Gu, Z. N.; Qin, Q. Z. *Chem. Phys. Lett*. **1999**, *300*, 739.
(14) Ding, F.; Fu, Z. W.; Qin, Q. Z. *Electrochem. Solid-State Lett.* **1999**, *2*, 418.
(15) Zheng, L. S.; Huang, R. B.; Li, W. Y.; Zhang, P.; Zhou, M. Y. *Chin. J. Chem. Phys*. **1992**, *5*, 369.
(16) Macklin, W. J.; Neat, R. J. *Solid State Ionics* **1992**, *153*−*56*, 694.
(17) Hjelm, A.; Granquist, C. G.; Wills, J. M. *Phys. Rev*. **1996**, *B54*, 2436.
(18) Fu, Z. W.; Kong, J. L.; Qin, Q. Z. *Sci. China, Ser. B* **1999**, *42*, 493.
(19) Fu, Z. W.; Kong, J. L.; Qin, Q. Z. *J. Electrochem. Soc*. **1999**, *146*, 3914.
(20) Mackrodt, W. C. *J. Solid State Chem.* **1999**, *142*, 428.
(21) Wang, S. L.; Ledingham, K. W. D.; Singhal, R. P. *J. Phys. Chem*. **1996**, *100*, 11282.
(22) Frisch, M. J.; Trucks, G. W.; Schlegel, H. B.; Gill, P. M. W.; Johnson, B. G.; Robb, M. A.; Cheeseman, J. R.; Keith, T. A.; Petersson, G. A.; Montgomery, J. A.; Raghavachari, K.; Al-Laham, M. A.; Zakrzewski, V. G.; Ortiz, J. V.; Foresman, J. B.; Peng, C. Y.; Ayala, P. Y.; Wong, M. W.; Andres, J. L.; Replogle, E. S.; Gomperts, R.; Martin, R. L.; Fox, D. J.; Binkley, J. S.; Defrees, D. J.; Baker, J.; Stewart, J. P.; Head-Gordon, M.; Gonzalez, C.; Pople, J. A. *Gaussian 94*, Revision E.3; Gaussian, Inc.: Pittsburgh, PA, 1995.
(23) Moller, C.; Plesset, M. S. *Phys. Rev.* **1934**, *46*, 618.
(24) Becke, A. D. *J. Chem. Phys.* **1993**, *98*, 5648.
(25) Lee, C.; Yang, W.; Parr, R. G. *Phys. Rev. B* **1988**, *37*, 785.
(26) Wachters, A. J. H. *J. Chem. Phys.* **1970**, *52*, 1033.
(27) Hay, P. J. *J. Chem. Phys.* **1977**, *66*, 4377.
(28) Reed, A. E.; Curtiss, L. A.; Weinhold, F. *Chem. Rev.* **1988**, *88*, 899.
(29) Foresman, J. B.; Head-Gordon, M.; Pople, J. A.; Frisch, M. J. *J. Phys. Chem.* **1992**, *96*, 135.